Reacting Fluids Laboratory
Department of Chemical Engineering
Louisiana State University
Baton Rouge, Louisiana

STATUS REPORT

on

EXPERIMENTAL VERIFICATION OF THE NON-EQUILIBRIUM MODEL FOR PREDICTING BEHAVIOR IN THE CHAR ZONE OF A CHARRING ABLATOR

N.A.S.A. Grant NGR 19-001-016

Evaluation of the Energy Transfer
in the Char Zone During Ablation

by

Gary C. April, Graduate Associate
Ralph W. Pike, Associate Professor
Principal Investigator
Eduardo G. del Valle, Graduate Associate

NASA - RFL - 8

July 1, 1968

Reacting Fluids Laboratory
Department of Chemical Engineering
Louisiana State University
Baton Rouge, Louisiana

STATUS REPORT

on

EXPERIMENTAL VERIFICATION OF THE NON-EQUILIBRIUM MODEL FOR PREDICTING BEHAVIOR IN THE CHAR ZONE OF A CHARRING ABLATOR

N.A.S.A. Grant NGR 19-001-016

Evaluation of the Energy Transfer
in the Char Zone During Ablation

by

Gary C. April, Graduate Associate
Ralph W. Pike, Associate Professor
Principal Investigator
Eduardo G. del Valle, Graduate Associate

NASA - RFL - 8

July 1, 1968

TABLE OF CONTENTS

FIGURES

TABLES

I. SUMMARY

A summary of the experimental results used for verification of the non-equilibrium model for predicting the behavior in the char zone of a charring ablator is presented. Mass flux values of the simulated pyrolysis gas were reduced by one to three orders of magnitude (0.05 lb/ft^2-sec nominal value) to increase the reactivity of the system at a 2000°F front surface temperature. Very good agreement was obtained over the entire experimental range. The effect of front surface temperature on reactivity is also presented.

A comparison of simulated chars (graphite and carbon) with the low density phenolic-nylon chars obtained from the Langley Research Center arc jets indicated good agreement and support for the simulation materials from a chemical viewpoint. Noted differences in the physical behavior was observed because of variations in the material pore size, density and porosity.

Air injection at the front surface of phenolic-nylon chars at a mass flux value of 0.035 lb/ft^2-sec without pyrolysis gas flow counter to the air indicated that there is oxygen breakthrough at the back surface. Additional studies with pyrolysis gas flow counter to the air injection at the surface is in progress.

II. INTRODUCTION

The primary objective of this research program is to determine accurately the energy absorbed in the char zone of a charring ablator, and how this is affected by the chemical reactions that take place in the char zone. Presently, there are two methods available to describe the limits on the heat transfer in the char zone. These are referred to as the frozen flow and equilibrium flow cases.

The minimum amount of energy that can be absorbed in the char zone can be computed by considering the flow to be frozen. This refers to the situation where the degradation products flowing through the char do not undergo any chemical reactions (the composition is constant). The amount of energy absorbed is given by the change in sensible heat of the gases.

The maximum amount of energy that can be absorbed in the char zone is obtained by considering the chemical species in the flow field to be in thermodynamic equilibrium. This refers to the situation where the degradation products undergo reaction at an infinitely fast rate, and the amount of energy absorbed is computed by considering the species to be in thermodynamic equilibrium. This gives the maximum energy absorbed since the reactions are nearly all endothermic.

The limits on the energy transfer established by these two cases have been previously reported (1,2). It was found that the amount of energy that could be absorbed was almost an order of magnitude greater for equilibrium flow than for frozen flow for the same front and back surface temperatures on the char. Due to the high mass flux of gases from the plastic decomposition the actual amount of energy that is absorbed lies somewhere between these two limiting cases and is determined

by the rates of chemical reaction among the species present.

In this report comparisons are made between experimental results obtained on the Char Zone Thermal Environment Simulator and the various models discussed in previous research (3). Several experiments using actual char specimens from low density phenolic-nylon composites obtained from the Langley Research Center were performed using a simulated pyrolysis gas mixture. Mass flux values were varied over a range of 3×10^{-5} to 2×10^{-2} lb/ft^2-sec to obtain a variety of reactive conditions. A range of front surface temperatures from 2000 to 2200°F was achieved in the apparatus.

Additional experiments using simulated char specimens of graphite and carbon (various grades) were made. After some preliminary mechanical difficulties these materials gave comparable results to the actual char specimens.

Air oxidation experiments were made to study the depth of oxygen penetration within the char. At the conditions studied, oxygen was observed in the exit stream indicating complete penetration through the chars. There was no pyrolysis gas flow blocking the oxygen injected at the front surface in these experiments.

III. ENERGY AND MOMENTUM TRANSFER IN NON-EQUILIBRIUM FLOW

To compute the energy transferred and the pressure distribution in the char zone, it is necessary to solve the energy equation and momentum equation with appropriate boundary conditions. For steady flow of degradation products in a char zone of constant thickness, the energy equation has the following form:

$$Wg.\bar{C}_p.\epsilon.\frac{dT}{dz} = \frac{d}{dz}\left[k_e.\frac{dT}{dz}\right] + \sum_{i=1}^{K+1} H_i R_i = 0 \qquad (1)$$

The first term represents the convective heat transfer, the second term represents conductive heat transfer and the third term represents the heat absorbed by chemical reactions. The derivation of this equation and a description of the numerical solution is given in reference (3).

To describe the pressure distribution a modified form of Darcy's equation was used which accounts for inertial effects that are important due to the high mass flux of degradation products. For the steady flow of an ideal gas in the char with varying mass flux, the following integral equation was obtained to predict the pressure distribution:

$$P = \left\{P_L^2 + 2R\left[\epsilon/\gamma\int_Z^L (W_g \mu T/\bar{M})\,dz + \beta\int_Z^L (Wg^2 T/\bar{M})\,dz\right]\right\}^{1/2} \qquad (2)$$

The first term on the right hand side is the pressure on the high temperature surface of the char, and the second and third terms represent the pressure loss due to viscous and inertial effects respectively.

The energy absorbed in the char zone is equal to the difference between the heat flux at the high temperature surface and the heat flux at

the low temperature surface. For non-equilibrium flow in the char this value is given by:

$$q_{cz} = \epsilon \sum_{i=1}^{K} \int_{T_o}^{T_L} WgX_i C_{Pi} dT + \sum_{i=1}^{K+1} \int_{T_o}^{T_L} \left[\frac{H_i R_i}{dT/dz}\right] dT \qquad (3)$$

The first term on the right hand side represents the heat absorbed due to the change in enthalpy of the gases and the second term represents the heat absorbed by chemical reactions.

Equations (1), (2), and (3) were solved numerically using programs written in FORTRAN IV on an IBM 7040 computer. This is described in detail in reference (3) where flow diagrams of the subprograms are given with a detailed print-out of the programs.

However before the calculations can be performed two additional pieces of information must be known. These are the specific chemical reactions that occur in the char with their associated kinetic constants and the initial composition of the degradation products when they enter the char zone. The nine specific chemical reactions, along with the corresponding frequency factor and activation energy data, that are thought to occur in the char zone over the reported temperature range are listed in Table 1. The initial composition is based on the composition predicted by thermodynamic equilibrium calculations and pyrolysis gas chromotography experiments and are presented in Table 2.

In Figure 1 a comparison is shown of the temperature distribution for non-equilibrium, equilibrium and frozen flow from the solution of the equations of change (continuity, momentum and energy) for a surface temperature of 2000°F and a mass flux of 0.05 lb/ft^2-sec. As shown the temperature distribution for non-equilibrium flow is only slightly less than that for frozen flow. However, the temperature distribution for equilibrium

TABLE 1

IMPORTANT CHEMICAL REACTIONS IN THE CHAR ZONE IN THE TEMPERATURE RANGE FROM 500 To 2500°F

REACTIONS	FREQUENCY FACTOR Sec^{-1}	ACTIVATION ENERGY Kcal
1. $CH_4 = \frac{1}{2} C_2H_6 + \frac{1}{2} H_2$	7.6×10^{14}	95.0
2. $C_2H_6 = C_2H_4 + H_2$	3.1×10^{13}	64.1
3. $C_2H_4 = C_2H_2 + H_2$	2.6×10^{8}	40.0
4. $C_2H_2 = 2\ C + H_2$	2.1×10^{10}	10.0
5. $C_6H_6 = 3\ C_2H_2$	1.4×10^{9}	52.0
6. $C + H_2O = CO + H_2$	9.3×10^{3}	70.0
7. $C + CO_2 = 2\ CO$	1.2×10^{12}	85.0
8. $NH_3 = \frac{1}{2} N_2 + \frac{3}{2} H_2$	2.8×10^{6}	60.8
9. $CH_4 + 2\ O_2 = CO_2 + 2\ H_2O$	1.5×10^{17}	30.2

TABLE 2

INITIAL FEED BLEND COMPOSITIONS SIMULATING THE PYROLYSIS GAS MIXTURE AT THE BACK SURFACE

GAS COMPONENT	MOLE PERCENT FEED BLEND #1	FEED BLEND #2	FEED BLEND #3
METHANE	32.5	43.6	46.3
HYDROGEN	37.2	35.0	31.7
NITROGEN	15.5	13.6	14.0
CARBON DIOXIDE	6.6	2.9	2.5
CARBON MONOXIDE	8.2	4.9	5.5
	100.0	100.0	100.0

INDEX OF EXPERIMENTS USING THE SPECIFIC FEED BLENDS LISTED ABOVE:

FEED BLEND #1: I, II, III, IV, V
FEED BLEND #2: VII, VIII, IX, XI, XII
FEED BLEND #3: XIII, XIV, XV, XVI

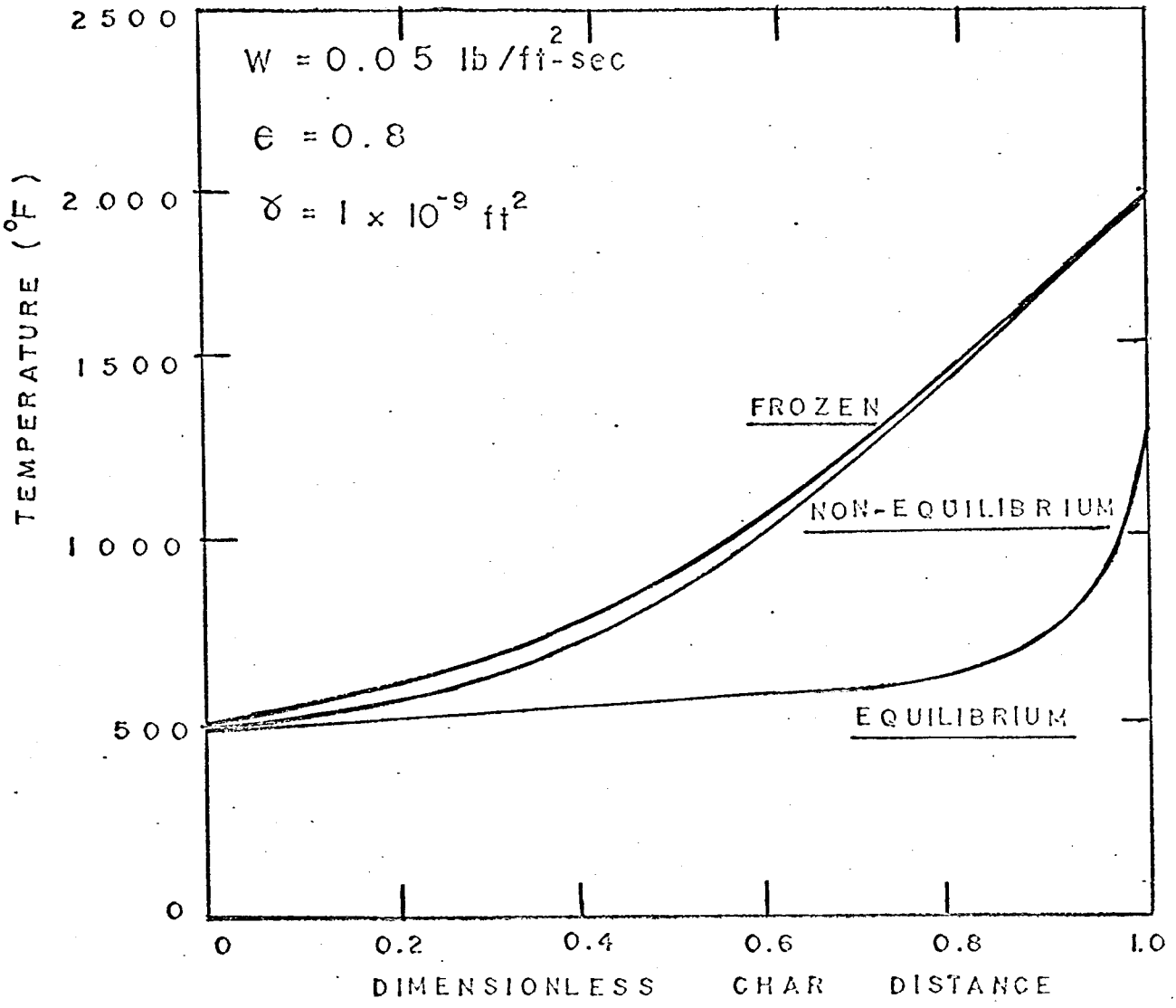

MODEL	SURFACE HEAT FLUX BTU/ft²-sec	PRESSURE DROP LB/ft²	MIDPOINT TEMPERATURE °F
FROZEN	44.67	15.3	948.7
NON-EQUILIBRIUM (9 REACTIONS)	45.17	15.1	890.6
EQUILIBRIUM	180.83	9.22	537.6

FIGURE 1
COMPARISON OF THE SOLUTIONS OF THE ENERGY EQUATION FOR FROZEN, EQUILIBRIUM AND NON-EQUILIBRIUM FLOW TO 2000 °F

flow is significantly different than that for frozen and non-equilibrium flow. Similarly, a comparison of the surface heat flux indicates that flow is essential frozen at the above conditions.

IV. EXPERIMENTAL SIMULATION OF THE CHAR ZONE DURING ABLATION

Char Zone Thermal Environment Simulator

Experiments were conducted to establish the accuracy of the non-equilibrium flow model with a system that simulates the char zone during ablation. A schematic diagram of the Char Zone Thermal Environment Simulator is shown in Figure 2.

In this simulator actual low density phenolic-nylon chars formed in the large arc jets at the Langley Research Center are mounted in a char holder. Chars are removed from 3 inch diameter arc jet samples, and saureisen cement is poured around the sides of the char inside a mold. This mounts the char with front and back surface exposed in a uniform inert ceramic casing which is mounted in the char holder. The holder is constructed of concentric tubes so gases of compositions that are typical of the degradation products can flow through the char as they would have on leaving the decomposition zone (Figure 3).

To have a temperature profile comparable to that on re-entry a bank of nine General Electric 1200 T3/CL quartz lamps are used to heat the char surface. The bank is located about 1-1/2 inches from the char surface, is surrounded by a reflector, and has a total output of about 15 KW. Various front surface temperatures are obtainable using the lamp chart in Table 3.

A total radiation pyrometer (Leeds and Northrup, Narrow Angle Rayotube) is focused on the front surface of the char through the bank of lamps to give an accurate measure of the front surface temperature. This is recorded on a strip chart recorder. The accuracy ($\pm$ 20°F at 2000°F) was estabished by comparing the temperature measured by the total radiation

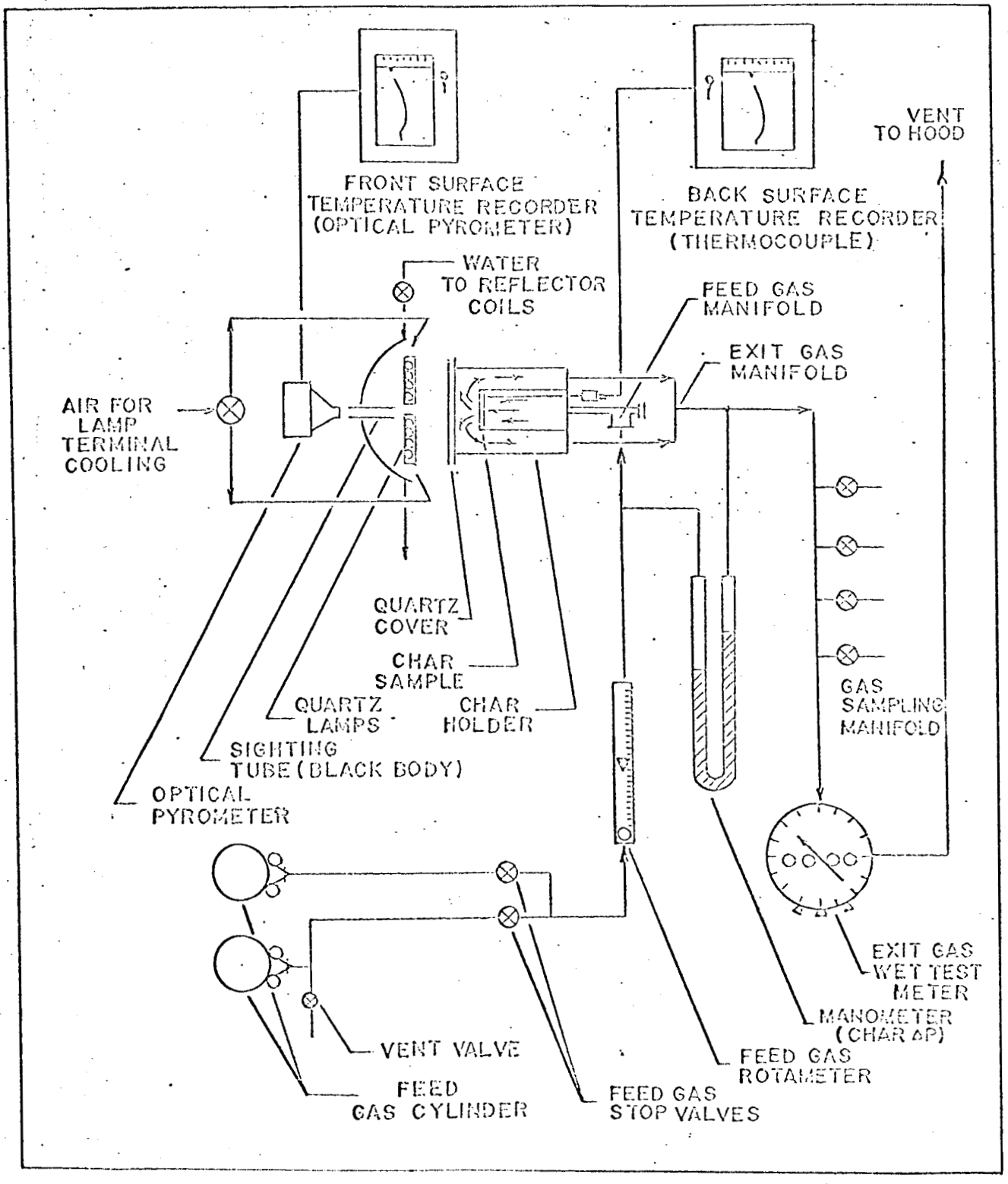

FIGURE 2

CHAR THERMAL ENVIRONMENT SIMULATOR

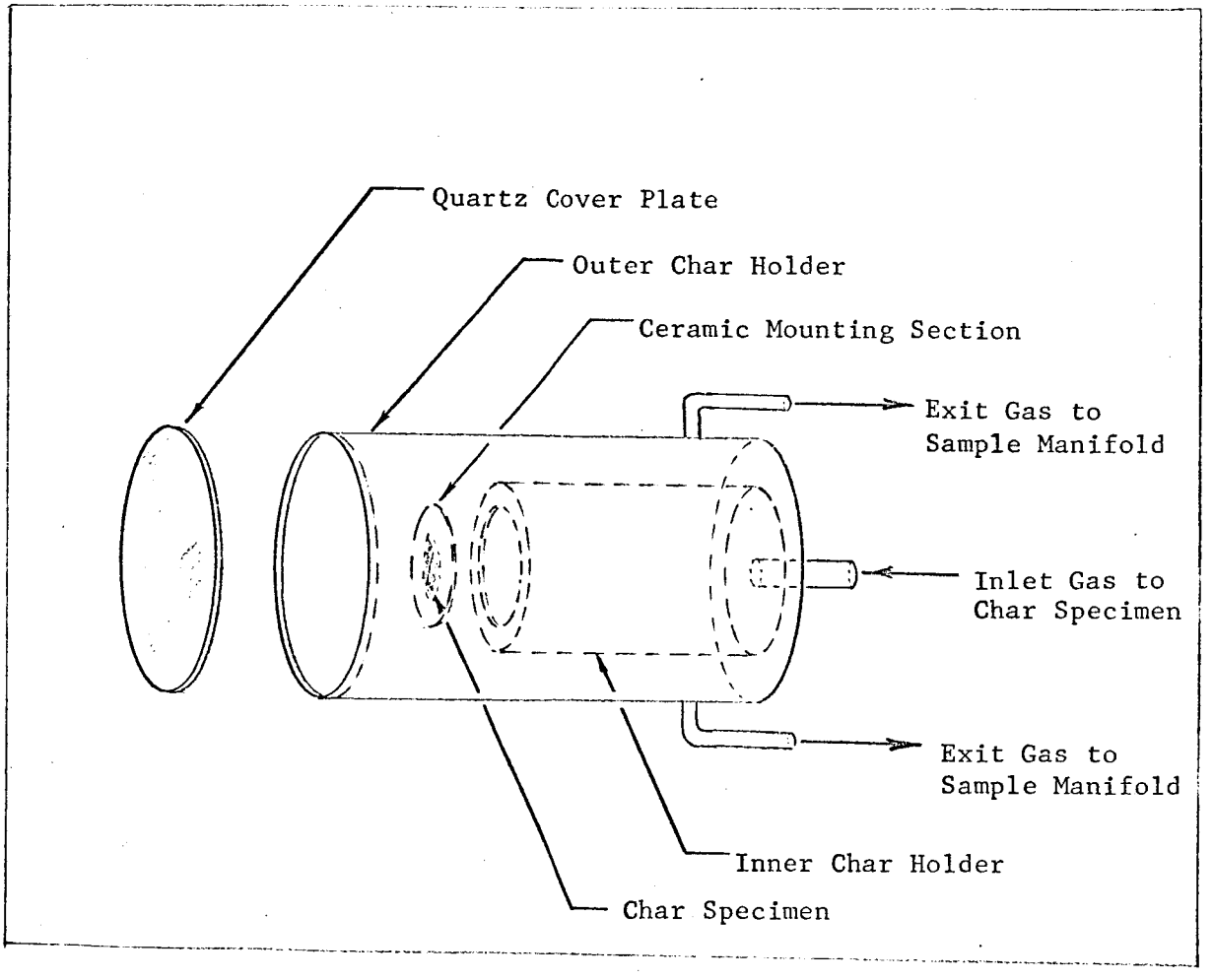

FIGURE 3

SCHEMATIC DIAGRAM OF THE CHAR SPECIMEN HOLDER AND THE ASSOCIATED SECTIONS

TABLE 3

COMPARISON OF LAMP REQUIREMENTS FOR A SPECIFIC FRONT SURFACE TEMPERATURE

LAMP TYPE	QUANTITY	RATED VOLTAGE, v	OPERATING VOLTAGE, v	RANGE OF TEMPERATURE	EXPERIMENT NUMBER
G.E. 1000 T3/CL	15	220	204	1350-1750°F	I-XII
G.E. 500 T3/CL	15	110	204	1550-1800°F	XIII-XV
G.E. 1200 T3/CL	9	144	204	1800-2150°F	XVI-XVII

All of the above lamps are quartz infrared lamps (detailed description in General Electric Catalog TP-116).

pyrometer with that of a calibrated optical pyrometer. Also it was established that the pyrometer was not being affected by sighting through the quartz lamps. The usual corrections to the measured temperature due to the reflected radiation from the lamps were made. This correction was less than 25°F at a char surface temperature of 1650°F.

The back surface temperature is measured with a shielded iron-constantan thermocouple and recorded on a strip chart recorder. The thermocouple makes firm contact with the char surface to insure an accurate surface temperature measurement. The thermocouple responds very rapidly when the bank of heating lamps is turned on indicating that good contact is being made between the char surface and the thermocouple tip.

A mixture of gases simulating the composition of the degradation products is prepared in a high pressure cylinder. The gas is passed through a regulator and is metered by a calibrated rotameter to the char holder. Having passed through the char the gases flow through a sample manifold where periodic samples are taken for gas chromatographic analysis and then through a wet test meter where volume (flow rate) is measured.

The composition of the feed and products are analyzed on a Packard Instrument Corporation gas chromatograph with a thermal conductivity detector. Hydrocarbons and carbon dioxide are determined on a twelve foot column filled with Porapak S packing with helium as a carrier gas. Nitrogen, oxygen and carbon monoxide are determined on a six foot column packed with 5A molecular sieve with helium as a carrier gas. Hydrogen is determined on this column using argon as a carrier gas.

The pressure drop across the char is measured with a U-tube manometer using water as the manometer fluid. The taps of the manometer are located

on the entrance and exit gas lines. The actual pressure drop across the char is determined by substracting from the total pressure drop, the pressure drop measured without the char in place.

The operating procedure consists of a start-up phase, a steady state phase, and a shut-down phase. In the start-up phase cooling water and air flow rates are adjusted, recorders are started, helium flow through the char is set and then power is applied to the bank of lamps. The temperature of the system rises to a steady-state value. In the steady-state phase at these conditions a set of data are collected which represents frozen flow in the char. Then the flow is switched to a feed of a composition typical of the degradation products. When temperature transients have damped, product samples are taken at five minute intervals for a run time of more than fifteen minutes. Operating conditions are then changed to obtain another set of data or the system is shut down.

To shut down the operation of the system, the flow through the char is changed to helium and then the power to the lamps is turned off. The system is allowed to cool to near room temperature and all of the flows are turned off.

V. EXPERIMENTAL RESULTS

A. Verification of Math Models

Experiments using actual char specimens from Langley Research Center are used to measure the ability of the models to predict actual behavior. As reported in previous research (3), for a mass flux value of 0.05 lb/ft^2-sec and a front surface temperature of 2000°F, a frozen flow condition exists. Therefore, because of the upper limit of 2000°F obtainable with the present experimental setup, a study at a variety of reduced mass flux values is necessary. In this way, residence times are increased and reactions observed at the maximum front surface temperature of 2000°F.

There are two indications that reactions are occuring from the analytical models. First, an increase in the surface heat flux for the non-equilibrium model above the frozen flow model approaching the upper limit of equilibrium flow value indicates reactivity. This indication has no experimental comparison, however, and offers no verifying results. The second and most important indication that a reaction has occurred is the change in exit gas composition. Values for the exit gas composition approximately equal to the inlet gas values indicate a frozen condition, whereas the degree with which these values deviate from the inlet gas values indicates the degree of reactivity. Once again the equilibrium composition is the upper limit. This latter indicator is used to verify the non-equilibrium flow model as adequate or inadequate in describing the flow system.

Two effects are illustrated to supplement the above discussion. In Table 4 a comparison of three experiments at constant mass flux (0.012-0.017 lb/ft^2-sec) is made for different front surfact temperatures (1575°F to 2035°F). As would be expected reactivity increases, as

TABLE 4

COMPARISON OF THE VARIOUS MODELS WITH EXPERIMENTAL RESULTS FOR THREE DIFFERENT VALUES OF THE MASS FLUX

RUN NUMBER	TEMPERATURE °F		GAS COMPONENT	EXIT GAS COMPOSITION, MOL %			
	FRONT	BACK		EXP.	NON-EQ FLOW	EQ. FLOW	FR. FLOW
XVI-49	2015 W = 0.00003	1259	HYDROGEN	84.5	84.70	82.13	31.7
			NITROGEN	4.2	3.84	9.52	14.0
			CARBON MONOXIDE	3.0	2.88	6.96	5.5
			CARBON DIOXIDE	0.6	0.00	0.00	2.5
			METHANE	7.7	8.21	1.20	46.3
			ETHANE	0.0	0.00	0.00	0.0
			ACETYLENE	0.0	0.00	0.00	0.0
XVI-48	2020 W = 0.0003	1120	HYDROGEN	55.2	52.46	82.60	31.7
			NITROGEN	10.5	9.16	9.48	14.0
			CARBON MONOXIDE	5.5	5.20	6.99	5.5
			CARBON DIOXIDE	1.4	0.84	0.00	2.5
			METHANE	27.3	30.17	0.83	46.3
			ETHANE	0.0	0.00	0.00	0.0
			ACETYLENE	0.1	2.15	0.00	0.0
XVI-50	2035 W = 0.0012	1262	HYDROGEN	53.2	51.26	83.19	31.7
			NITROGEN	10.7	9.09	9.43	14.0
			CARBON MONOXIDE	6.7	6.17	7.06	5.5
			CARBON DIOXIDE	0.2	0.32	0.00	2.5
			METHANE	29.2	29.55	0.31	46.3
			ETHANE	0.0	0.00	0.00	0.0
			ACETYLENE	10.1	3.57	0.00	0.0

indicated by exit gas composition and surface heat flux values, as the surface temperature increase. The experimentally determined exit gas compositions agree within experimental error to those calculated by the non-equilibrium flow model. The values calculated by the equilibrium model are in gross disagreement. This same result can be seen in Table 5 comparing surface heat flux for the various models.

A second effect is illustrated in Table 6 where varying mass flux values (3×10^{-5} - 2×10^{-2} lb/ft^2-sec) are compared for a constant front surface temperature (2035°F). A wide range of reactivity is noted with larger changes occurring at the low mass flux (or high residence time) values. In all cases good agreement between experimental and calculated exit gas compositions result. Table 7 contains the surface heat flux values for the various models.

Two deviations do occur on closer inspection, however, and these can be justified. The first results in the back surface temperature of experiment XVI-48 which is lower than the adjacent experimental values. This value is an average of temperatures in the non-steady state region during the initial phases of the experiment. The second occurs in high acetylene compositions in the exit gas stream predicted by the non-equilibrium model. This results from a very sensitive energy of activation on reaction 3 (Table 1) with temperature.

The important conclusion to reach is that the composition of the major constituents are predicted over a wide range of conditions varying from frozen flow to a highly reactive state.

TABLE 5

COMPARISON OF THE SURFACE HEAT FLUX AND THE PRESSURE DROP FOR FROZEN, EQUILIBRIUM AND NON-EQUILIBRIUM FLOW

Run Number	Temperature °F		Calculated Variables	Flow Model		
	Front	Back		Fr. Flow	Non.Eq. Flow	Eq. Flow
XVI-49	2015 W = 0.00003	1259	Pressure Drop lb/ft^2	0.0	0.0	0.0
			Surface Heat Flux Btu/ft^2-sec	0.02	0.06	0.26
XVI-48	2020 W = 0.0003	1120	Pressure Drop lb/ft^2	0.0	0.0	0.0
			Surface Heat Flux Btu/ft^2-sec	0.41	0.92	4.20
XVI-50	2035 W = 0.0012	1262	Pressure Drop lb/ft^2	0.5	0.5	0.8
			Surface Heat Flux Btu/ft^2-sec	0.67	0.78	13.77

TABLE 6

COMPARISON OF THE VARIOUS MODELS WITH EXPERIMENTAL
RESULTS FOR THREE DIFFERENT VALUES OF THE FRONT SURFACE TEMPERATURE

RUN NUMBER	TEMPERATURE °F		GAS COMPONENT	EXIT GAS COMPOSITION, MOL %			
	FRONT	BACK		EXP.	NON-EQ FLOW	EQ. FLOW	FR. FLOW
XVI-50	2035 W = 0.0012	1262	HYDROGEN	53.2	51.26	83.19	31.7
			NITROGEN	10.7	9.07	9.43	14.0
			CARBON MONOXIDE	6.7	6.17	7.06	5.5
			CARBON DIOXIDE	0.2	0.32	0.00	2.5
			METHANE	29.2	29.55	0.31	46.3
			ETHANE	0.0	0.00	0.00	0.0
			ACETYLENE	<0.1	3.57	0.00	0.0
XIV-42	1800 W = 0.0014	956	HYDROGEN	30.9	31.72	82.46	31.7
			NITROGEN	14.0	13.91	9.49	14.0
			CARBON MONOXIDE	6.1	5.83	6.99	5.5
			CARBON DIOXIDE	2.7	2.30	0.00	2.5
			METHANE	46.3	46.08	0.93	46.3
			ETHANE	0.0	0.00	0.00	0.0
			ACETYLENE	0.1	0.16	0.00	0.0
V-11	1575 W = 0.0017	728	HYDROGEN	37.7	37.20	70.59	37.2
			NITROGEN	15.5	15.50	11.54	15.5
			CARBON MONOXIDE	8.1	8.21	14.29	8.2
			CARBON DIOXIDE	6.4	6.59	0.26	6.6
			METHANE	31.5	32.50	2.19	32.5
			ETHANE	0.1	0.00	0.00	0.0
			ACETYLENE	0.6	0.00	0.00	0.0

TABLE 7

COMPARISON OF THE SURFACE HEAT FLUX AND THE PRESSURE DROP FOR FROZEN, EQUILIBRIUM AND NON-EQUILIBRIUM FLOW

Run Number	Temperature °F		Calculated Variables	Flow Model		
	Front	Back		Fr. Flow	Non.Eq. Flow	Eq. Flow
XVI-50	2035 W = 0.0012	1262	Pressure Drop lb/ft^2	0.5	0.5	0.8
			Surface Heat Flux Btu/ft^2-sec	0.67	0.78	13.77
XIV-42	1800 W = 0.0014	956	Pressure Drop lb/ft^2	0.3	0.3	0.4
			Surface Heat Flux Btu/ft^2-sec	0.55	0.56	12.75
V-11	1575 W = 0.0017	728	Pressure Drop lb/ft^2	0.4	0.4	0.5
			Surface Heat Flux Btu/ft^2-sec	0.68	0.68	13.07

B. Simulated Char Experiments Using Various Graphite and Carbon Materials

Additional experiments were made to determine whether graphite and carbon simulated the actual Langley arc jet char specimens. The large difference between the two is in porosity values and possibly higher path resistance in the graphite and carbon samples. Two specimens were studied in this phase of the program and there descriptions are listed in Table 8.

These specimens are obtained in three inch wide by six inch long by one inch thick block sections from which one inch diameter by one-fourth inch thick samples are made. A fine blade saw is used to cut the thichness and a hole saw used to cut the diameter.

A series of runs were made at conditions duplicating char specimen runs for overall comparison of results; i.e. exit gas composition and front and back temperatures. Inspection of the analytical data indicated a region near startup of increased methane and decreased hydrogen concentration with eventual leveling to normal behavior. These results were noted in replicate experiments to occur at or near the same run time and final concentration. Figures 4, 5 and 6 show the peak in the methane concentration (and the decline in hydrogen concentration) versus run time.

In reference 4 and 5 it is suggested that methane production is enhanced by passing hydrogen over finely granulated graphite (or carbon). The fine particles increase surface area per unit mass of material and therefore increases the reactive sites available for combination with hydrogen to form methane.

Several additional experiments were made with identically machined plugs followed by air (or nitrogen) sparging to eliminate trapped fines within the pore sites of the specimens. These experiments duplicated the Langley arc jet char experiments and eliminated the methane increase during the initial phases of the run. Figures 7 and 8 show typical run sheet

TABLE 8

DESCRIPTION OF SIMULATED CHAR SPECIMENS

SPECIMEN IDENTIFICATION	POROSITY (AREA VOIDS/TOTAL AREA)	DENSITY $16/FT^3$	AVERAGE PORE DIA., FT.	EXPERIMENT
GRAPHITE (GRADE 25)	0.47	64.4	0.0004	VIII
CARBON	0.55	--	--	IX
GRAPHITE (GRADE 45)	0.47	65.0	0.0019	XI
GRAPHITE (GRADE 25)	0.47	64.4	0.0004	XIII
GRAPHITE (GRADE 25)	0.47	64.4	0.0004	XV

FIGURE 4: RUN SHEET EXPERIMENT VIII

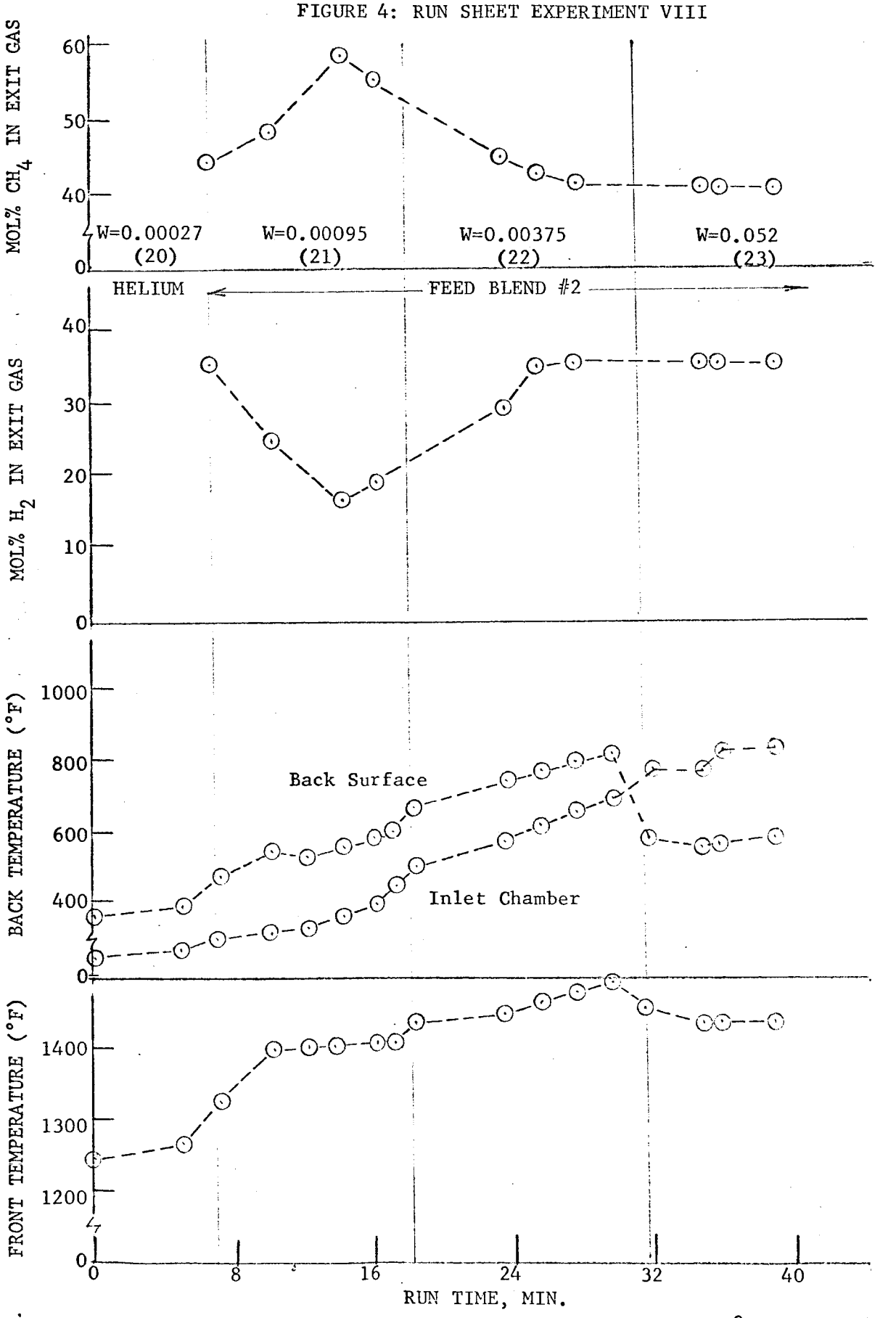

W in lb/ft^2-sec

( ) indicates run number

FIGURE 5: RUN SHEET EXPERIMENT IX

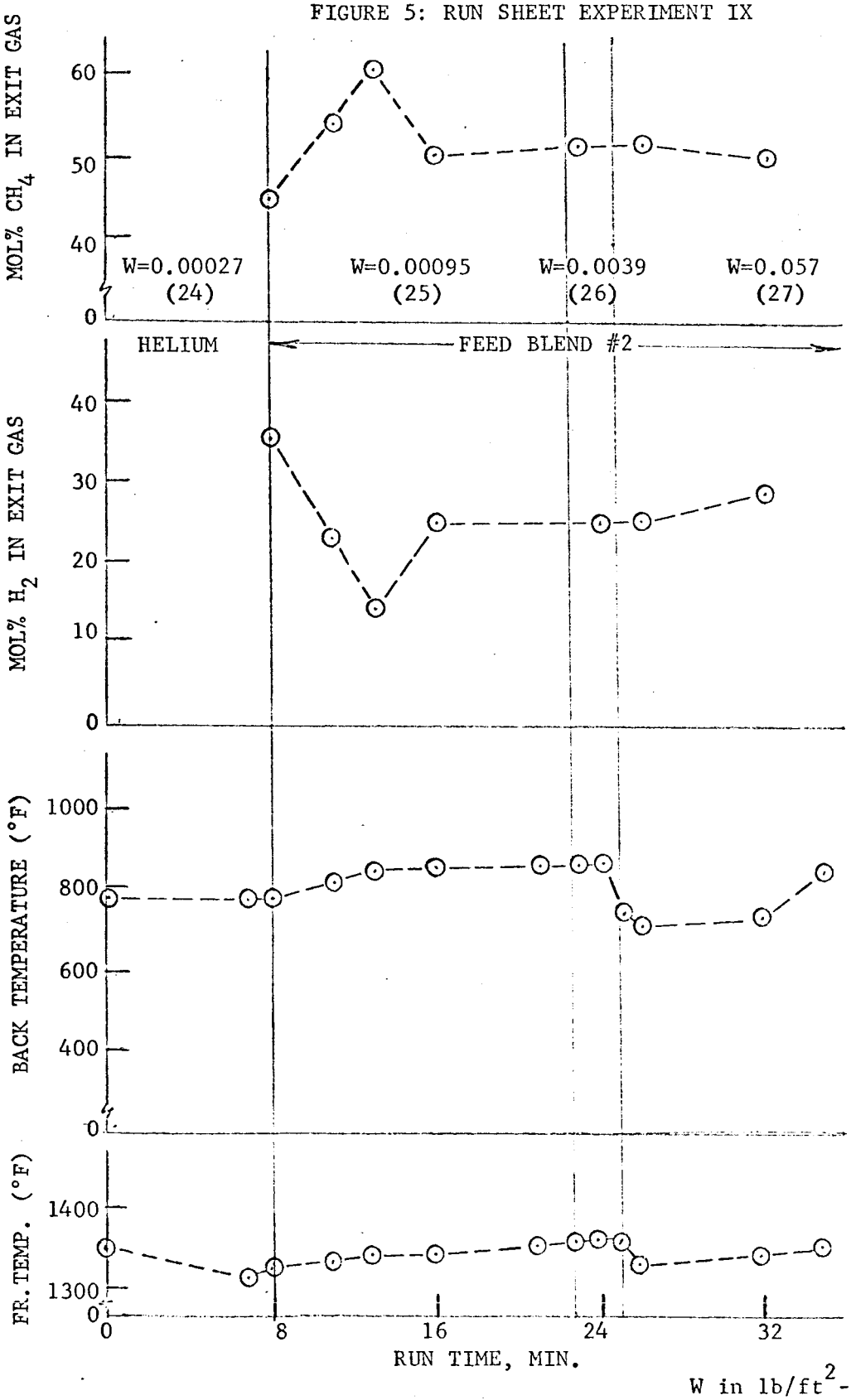

W in lb/ft^2-sec

( ) indicates run number

FIGURE 6: RUN SHEET EXPERIMENT XI

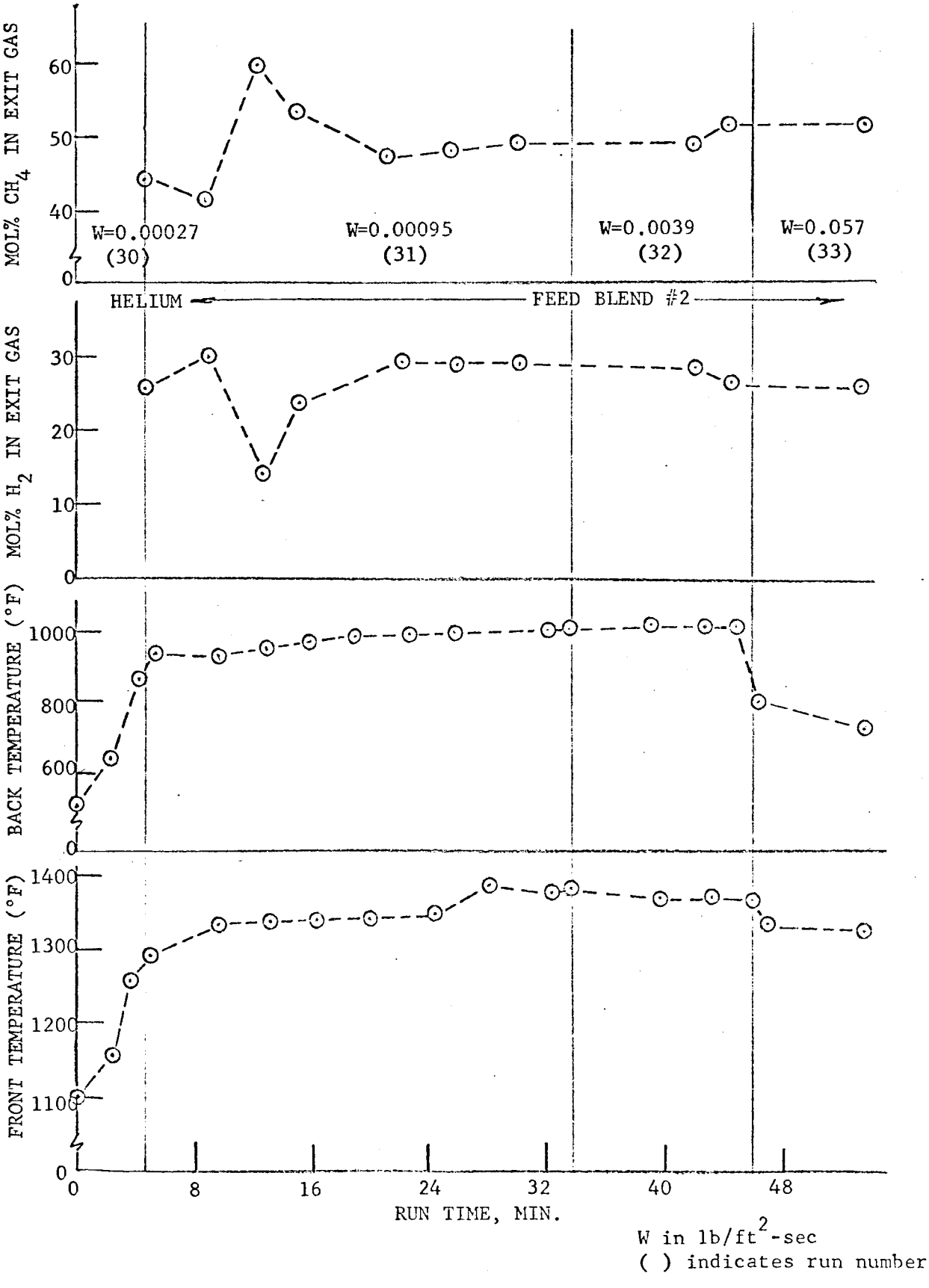

FIGURE 7: RUN SHEET EXPERIMENT XIII

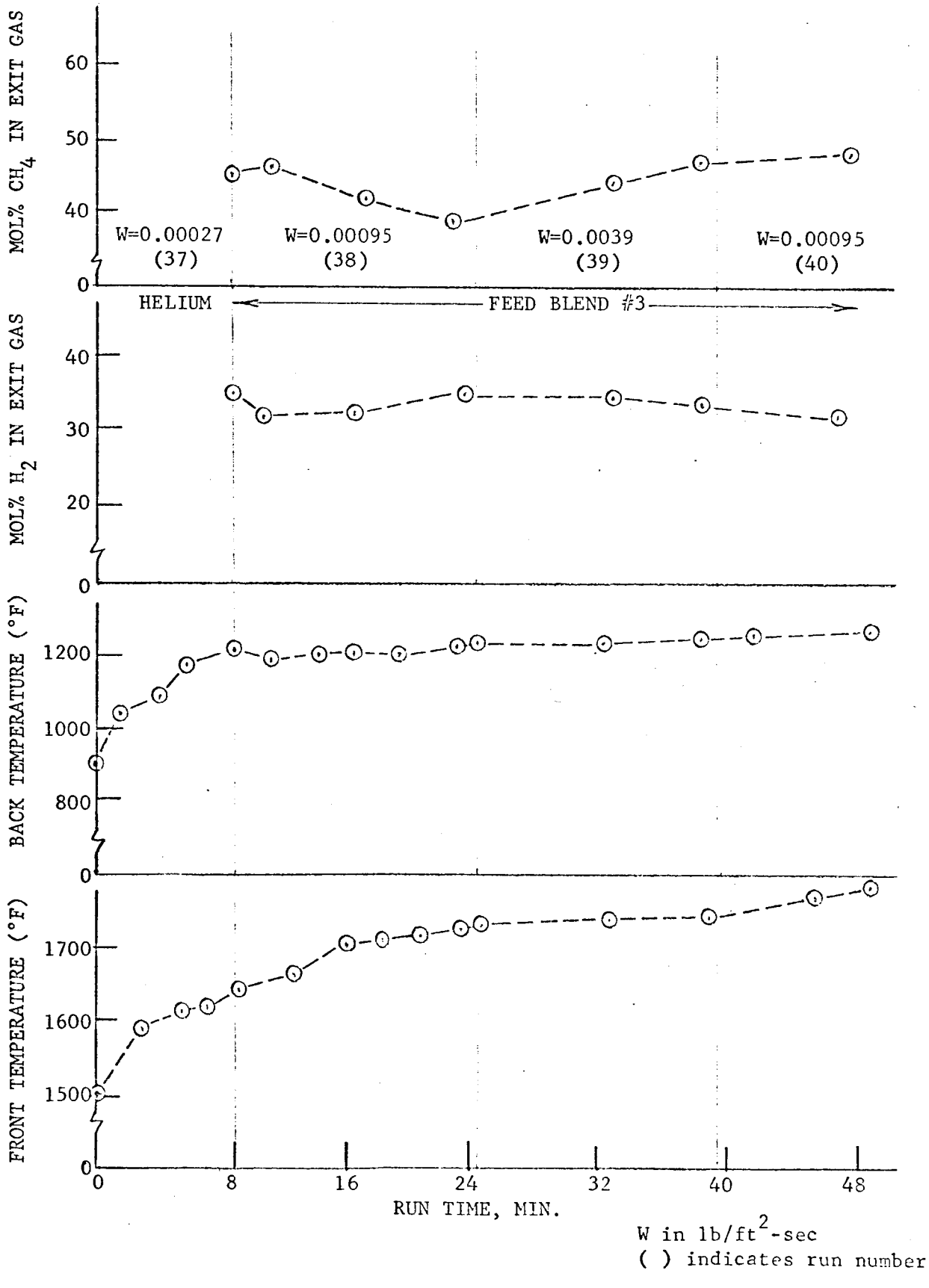

W in lb/ft^2-sec

( ) indicates run number

FIGURE 8: RUN SHEET EXPERIMENT V

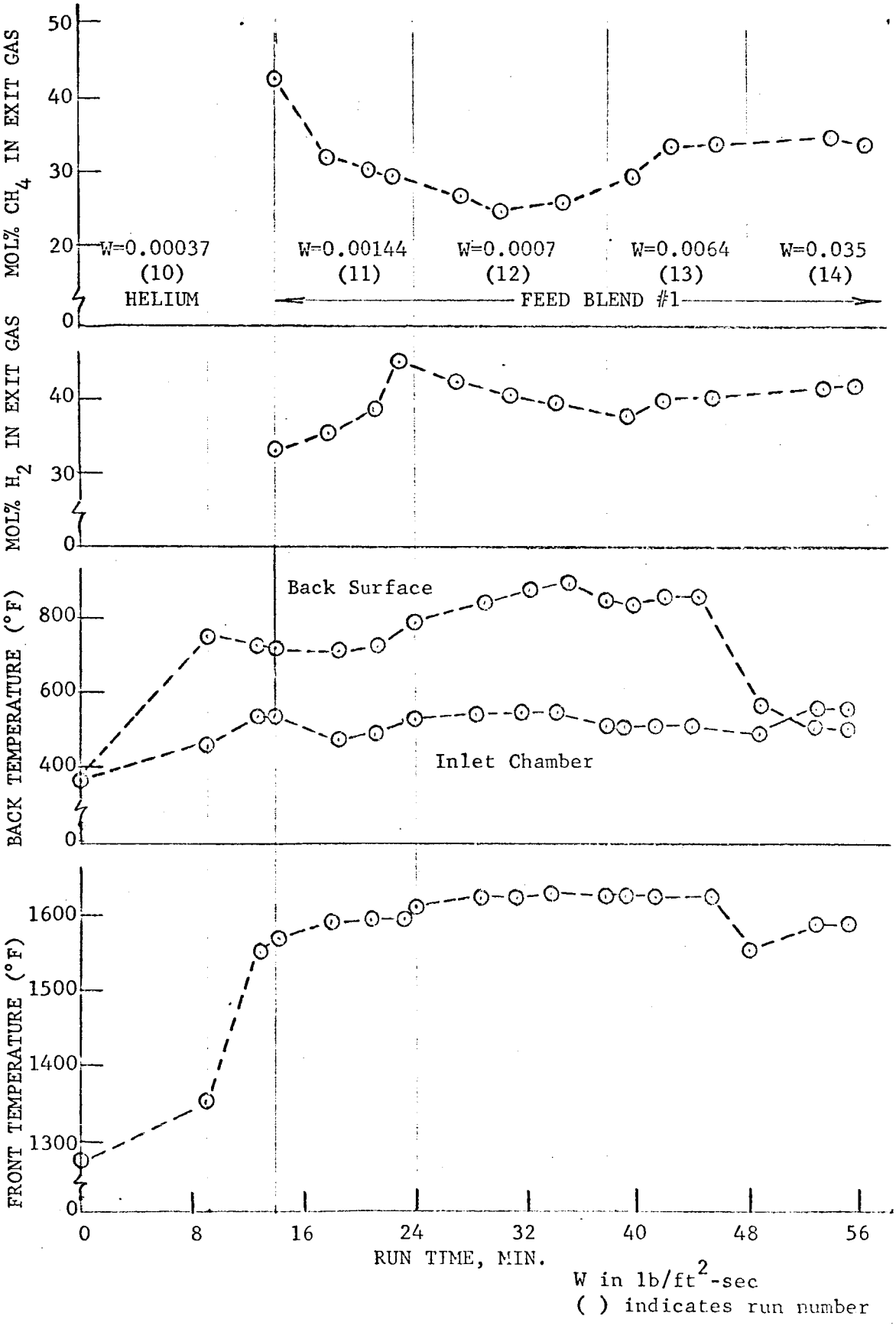

data for the graphite experiments, while Figures 9 and 10 are typical data for the Langley char experiments. The same overall trend is noted in the comparison. (Also in Figure 10, the large decrease in methane concentration is indicative of high reactivity at the low mass flux value.)

Therefore, for all practical purposes up to 2000°F, graphite and carbon simulate the char behavior from a chemical viewpoint, although certain physical property differences occur (i.e. pressure drop).

C. Air Penetration Studies

Two additional experiments were made to determine if oxygen injected at the front surface of the specimen penetrated the entire thickness of the specimen or was reacted completely within the char. The experiments performed were simplified by merely reversing the inlet and outlet gas lines. Compressed air was used as a feed gas and the flow was adjusted to obtain the desired oxygen mass flux. No pyrolysis gases were passed through the char from the back to the front surface as is the case in actual re-entry flights.

Results are shown in Figure 11 for an air mass flux value of 0.037 $lb/ft^2/sec$ and a front surface temperature of 2050°F. Steady state was achieved with helium flow before the air was allowed to flow into the char. Immediately after the air cut-in, the back surface temperature dropped due to the difference in molecular weights of the two feeds followed by a slight difference in pressure drop from 5.0 inches of water to 4.8 inches of water. The sample obtained during this period indicated 4% oxygen in the exit stream or total break through of oxygen to the back surface. Shortly thereafter a pressure drop decrease resulted (3.4 inches of water). This normally indicated possible cracking of the ceramic (inert) mounting ring or a severe crack in the specimen resulting in lower resistance to flow by channeling. Two additional samples of the

FIGURE 9: RUN SHEET EXPERIMENT XIV

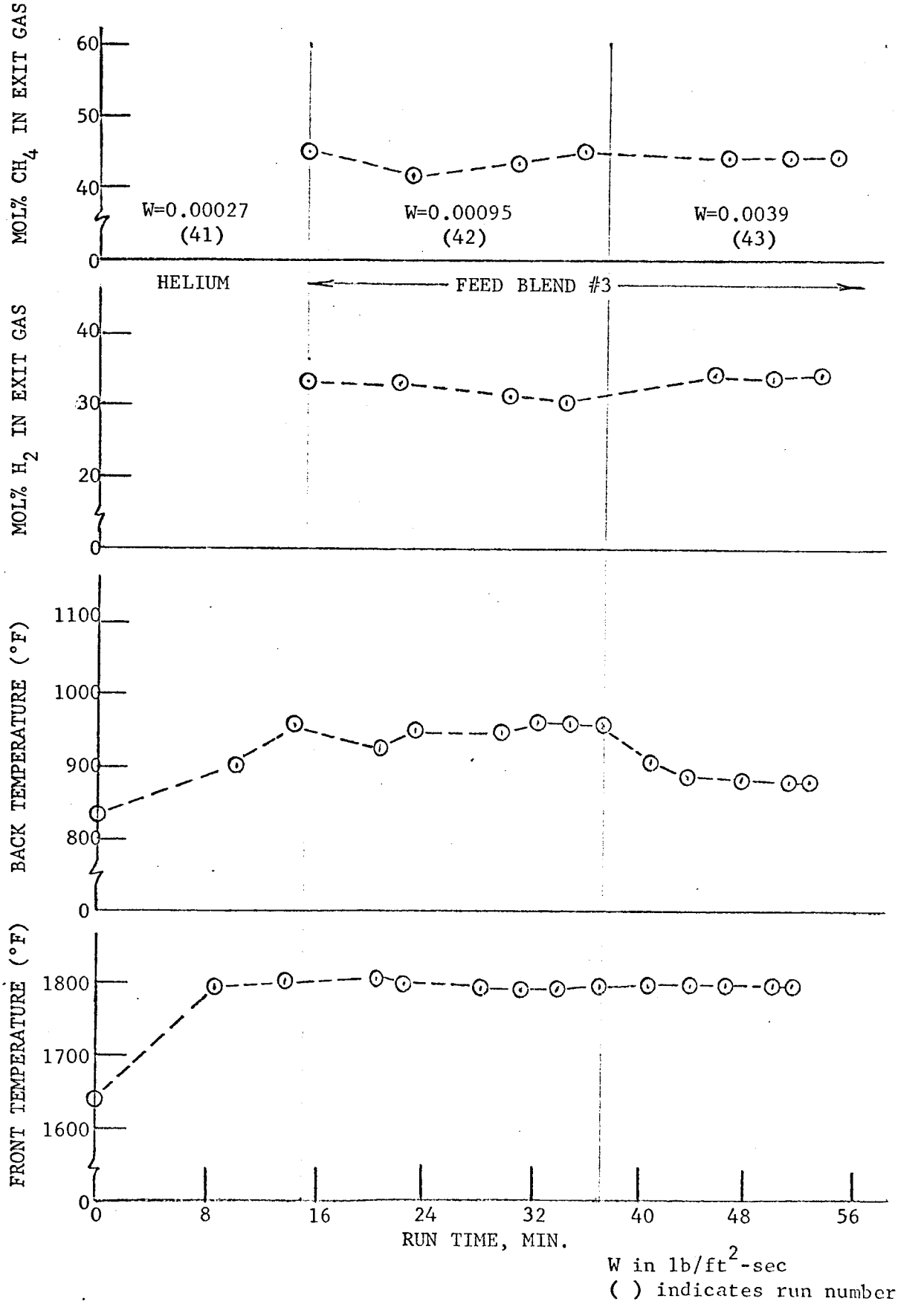

W in lb/ft^2-sec

( ) indicates run number

FIGURE 10: RUN SHEET EXPERIMENT XVI

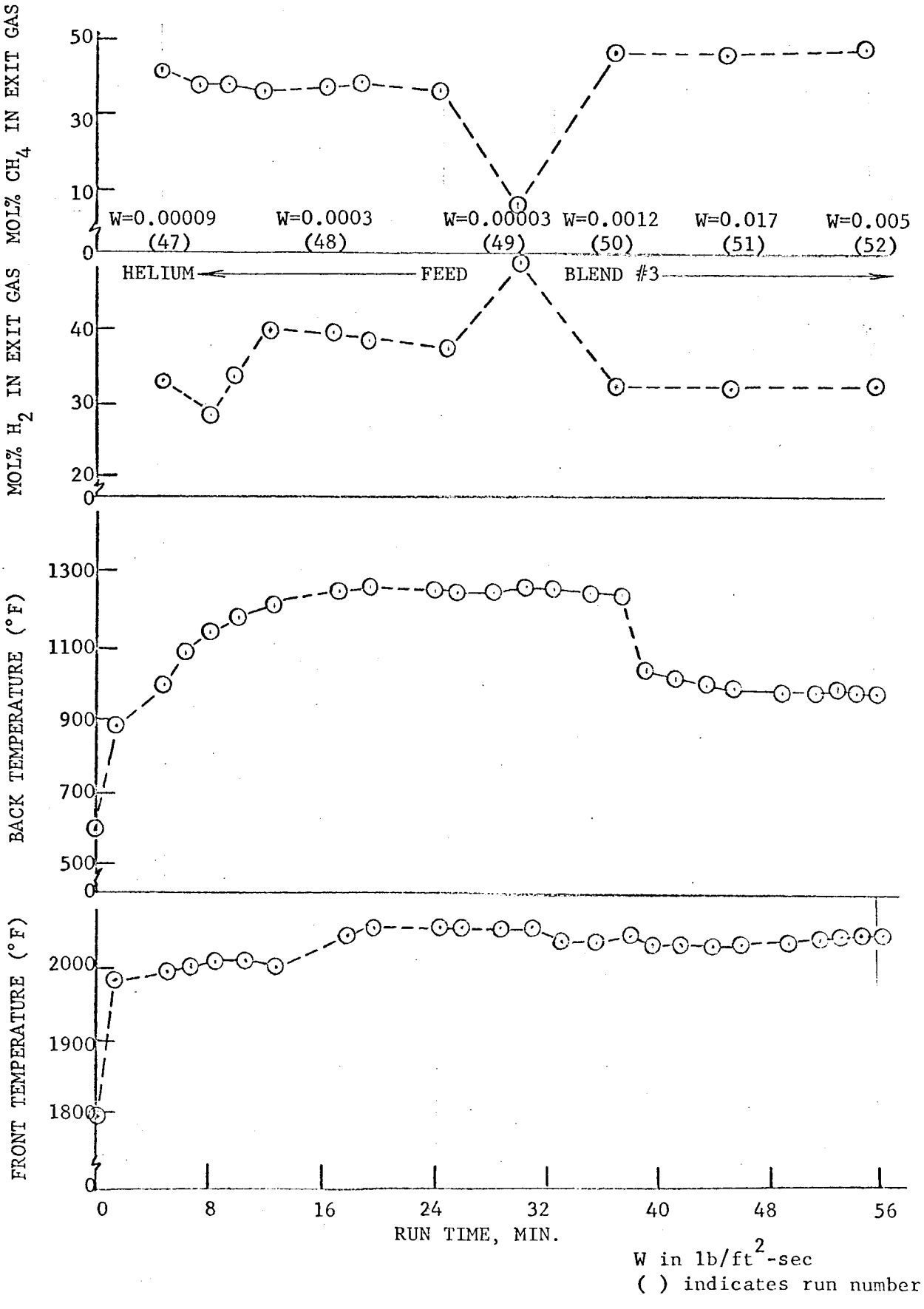

W in lb/ft^2-sec

( ) indicates run number

FIGURE 11: RUN SHEET EXPERIMENT XVII

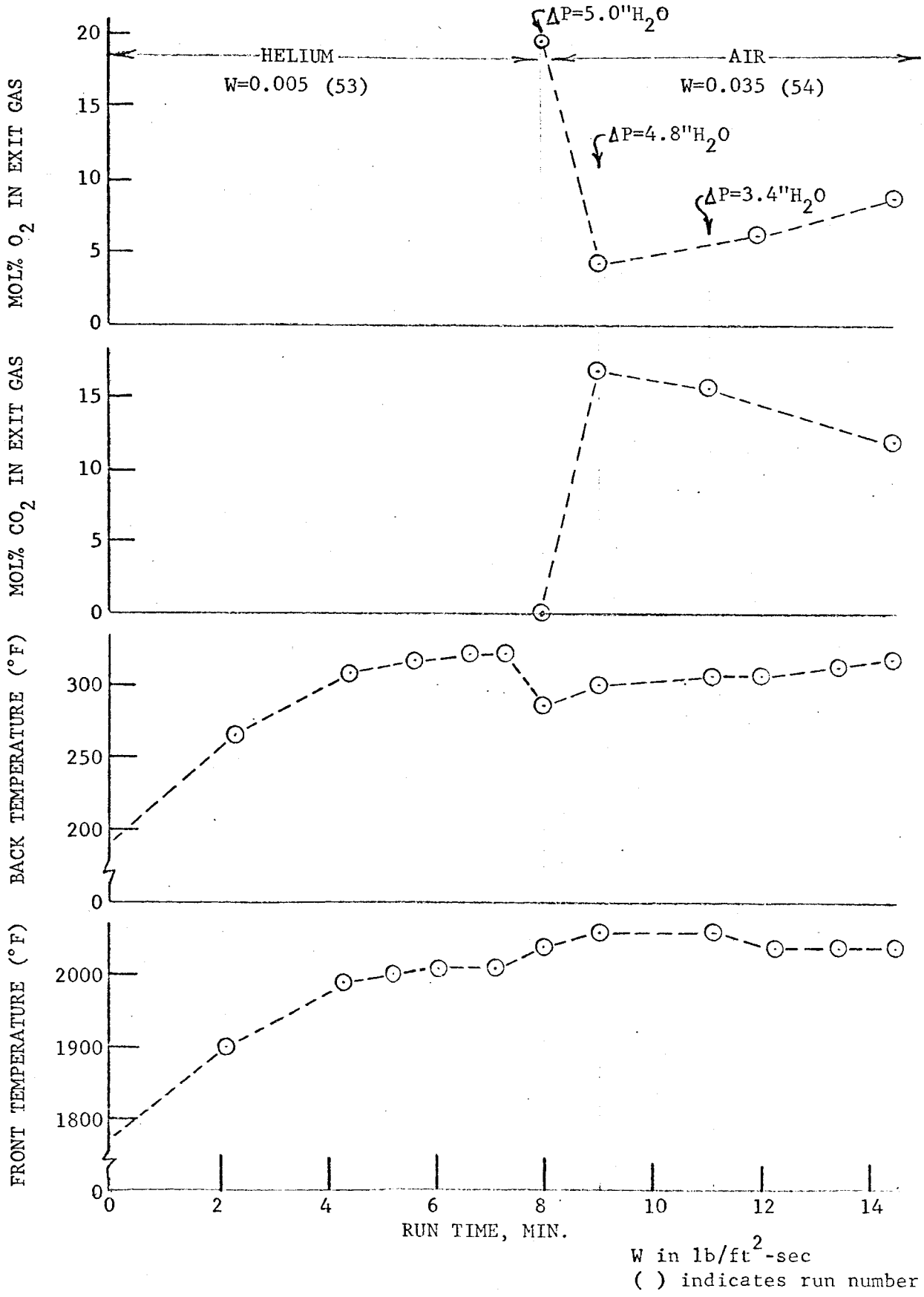

exit gas stream were taken and the experiment terminated. The remaining samples indicated higher oxygen concentration at the back surface and inspection of the char specimen revealed large erroded areas in the material (Figures 12 and 13). Prolonged running would have resulted in total reaction of the char noted in an earlier experiment.

Possible additional runs will be made with air injection parallel to the front surface with pyrolysis gas flow from back to front simulating the actual case expected during re-entry.

FIGURE 12: FRONT VIEW OF PHENOLIC-NYLON CHAR AFTER 3-5 MINUTES EXPOSURE TO AIR AT 0.035 lb/ft^2-sec AT 2035°F

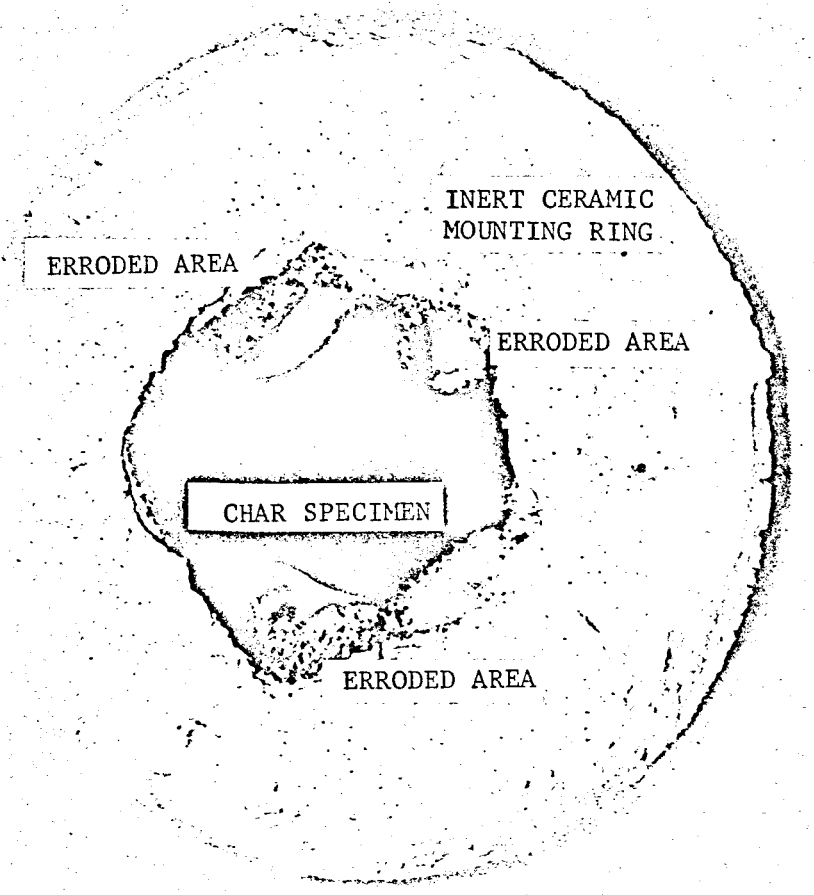

FIGURE 13: BACK VIEW OF PHENOLIC-NYLON CHAR AFTER 3-5 MINUTES EXPOSURE TO AIR AT 0.035 lb/ft^2-sec AT 2035°F

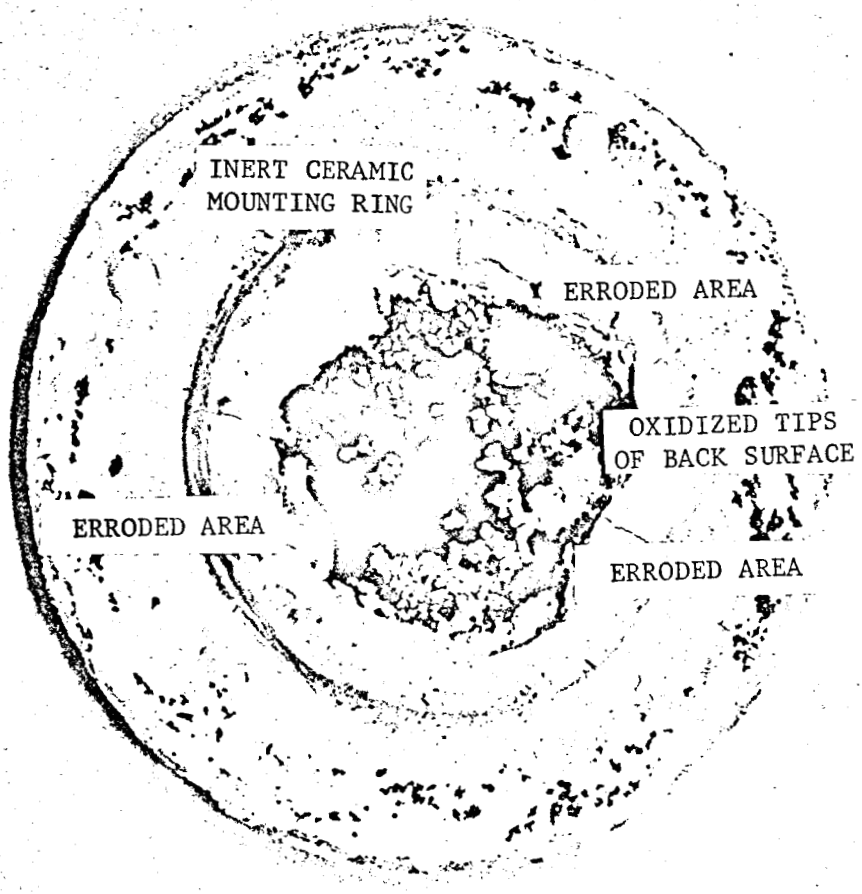

VI. FUTURE EXPERIMENTAL WORK

A. Better Pyrolysis Gas Composition

Recent work by Nelson and Sikes at L.R.C. indicate that high molecular weight species such as phenol, cresols, xylenol, etc. are present in significant quantities in the pyrolysis gas stream. Future experiments will attempt to combine a gas and liquid feed blend to more accurately simulate the pyrolysis gas composition. This will require the addition of liquid metering devices, preheat sections to vaporize the liquid feed stock and liquid knockout pots in the exit lines to trap any unreacted condensate.

B. Carbon 14 Tagging of Key Species

Carbon 14 tagged species will be included in the studies to pinpoint reactions expected to be important in this temperature region. The use of a liquid scintillation counter will be required for these additional analyses. Also important data regarding possible carbon deposition within the char will be obtained by slicing very thin layers of the char specimens with analysis of the materials for radioactivity. In this way the regions where deposition occur can be pinpointed and possible solid density vs. thickness plots can be obtained.

C. Catalyst Studies

The use of heterogeneous catalyst to possible enhance chemical reaction at milder conditions will be studied. These tests will hopefully indicate whether catalystic salting of the chars will result in beneficial heat adsorption or lesser amounts of material required to protect space vehicles.

VII. NOMENCLATURE

C_{p_i}	Heat capacity of specie i
$\bar{C}_p$	Average heat capacity of pyrolysis gas
H_i	Enthalpy per unit mass of specie i
k_e	Effective thermal conductivity
K	Number of gas species
L	Char thickness
$\bar{M}$	Average molecular weight of pyrolysis gas
P	Pressure
q	Heat flux
R	Universal gas constant
R_i	Reaction rate of specie i (moles/unit time/unit volume)
T	Temperature
W_g	Mass flux of pyrolysis gas in char pores
X_i	Mole fraction of specie i
Z	Char distance
γ	Permeability of char
ϵ	Porosity of char
μ	Viscosity of pyrolysis gas
β	Inertial coefficient in modified Darcy's Equation

Subscripts

C_Z	Char zone
i	Specie
0	Initial value
L	Final value (where Z = L)

VIII. REFERENCES

1. April, G. C., E. G. del Valle and R. W. Pike, "Transport Phenomena in the Char Zone I. Evaluation of the Energy Transfer for Frozen and Equilibrium Flow," Paper No. 13d National Meeting of the A.I.Ch.E., Salt Lake City, Utah (May 21-24, 1967).

2. April, G. C., E. G. del Valle and R. W. Pike, "Solution of the Frozen Flow Energy Equation," N.A.S.A. - R.F.L. - 2, Reacting Fluids Laboratory Status Report, Louisiana State University (July 1, 1966).

3. Pike, R. W., G. C. April, E. G. del Valle, "Reaction Kinetics in the Char Zone," N.A.S.A. - R.F.L. - 7, Reacting Fluids Laboratory Status Report, Louisiana State University (June 15, 1967).

4. King, A. B. and Henry Wise, "Reaction Kinetics of Hydrogen Atoms with Carbon Films," Journal of Physical Chemistry, vol. 67, no. 6 (June 14, 1963) p. 1163.

5. Gulbransen, E. A., K. F. Andrew, and F. A. Brassart, "The Reaction of Hydrogen with Graphite at 1200° to 1650°C," Journal of the Electrochemical Society, vol. 112, no. 1 (January 1965) p. 49.

IX. APPENDIX

This appendix contains a summary of all experimental results obtained on the Char Zone Thermal Environment Simulator with reference to specific run sheets contained in N.A.S.A. - R.F.L. - 8.

TABLE 9

A SUMMARY OF EXPERIMENTS

EXPERIMENT NO.	SPECIMEN IDENTIFICATION	RUN NO.	EXPERIMENTAL RUN CONDITIONS				REMARKS OR COMMENTS
			$\dot{W}$ (lb/ft^2-sec)	T_L (°F)	T_o (°F)	FEED BLEND	
I	LRC-C9-S46	1	0.00001-0.0002	1335	925	Helium	Test Equipment
II	LRC-C9-S46	2	0.0005	1250	890	Helium	Start Up
		3	0.0015	1280	790	No. 1	Equipment Check
		4	0.0006	1300	855	No. 1	Analytical Check
III	LRC-C10-S52	5	0.012-0.053	1160	160	Helium	Start Up
		6	0.0375	1225	250	No. 1	Analytical Check
		7	0.0205	1390	450	No. 1	Analytical Check
IV	LRC-C10-S52	8	0.0017	1305	555	Helium	Start Up
		9	0.0051	1550	760	No. 1	Run Sheet (Fig.14)
V	LRC-C10-S52	10	0.0004	1465	720	Helium	Start Up
		11	0.0014	1575	730	No. 2	
		12	0.0007	1604	784	NO. 2	Run Sheet (Fig. 8)
		13	0.0064	1610	770	No. 2	
		14	0.0350	1555	472	No. 2	
VI	LRC-C10-S52	15	0.0013	1530	830	Helium	Start Up
		16	0.0097	1595	750	No. 2	Analytical Problems
VII	LRC-C10-S52	17	0.0003	1580	625	Helium	Equipment Check
		18	0.0003	1590	630	Helium	Start Up
		19	0.0009	1730	705	No. 2	Run Sheet (Fig.15)

Note: All LRC identified specimens are low density phenolic-nylon chars from the Langley Research Center (NASA)

TABLE 9 (Continued)

EXPERIMENT NO.	SPECIMEN IDENTIFICATION	RUN NO.	EXPERIMENTAL RUN CONDITIONS				REMARKS OR COMMENTS
			W (lb/ft^2-sec)	T_L (°F)	T_o (°F)	FEED BLEND	
VIII	Graphite (Grade 25)	20	0.0003	1260	380	Helium	Start Up
		21	0.0009	1370	530	No. 2	
		22	0.0038	1470	740	No. 2	Run Sheet (Fig. 4)
		23	0.0520	1450	570	No. 2	
IX	Carbon	24	0.0003	1335	770	Helium	Start Up
		25	0.0009	1350	815	No. 2	
		26	0.0039	1370	800	No. 2	Run Sheet (Fig. 5)
		27	0.0570	1350	725	No. 2	
X	High Density Phenolic-Nylon	28	0.0008	1400	665	Helium	Start Up
		29	0.0057	1480	800	Air	Equipment Failure
XI	Graphite (Grade 45)	30	0.0003	1215	600	Helium	Start Up
		31	0.0009	1335	805	No. 2	
		32	0.0039	1390	865	No. 2	Run Sheet (Fig. 6)
		33	0.0570	1355	595	No. 2	
XII	Graphite (Grade 25)	34	0.0003	1305	720	Helium	Start Up
		35	0.0009	1400	930	No. 2	Analytical Problems
		36	0.0039	1350	920	No. 2	
XIII	Graphite (Grade 25)	37	0.0003	1567	1020	Helium	Start Up
		38	0.0009	1690	1210	No. 3	
		39	0.0039	1725	1220	No. 3	Run Sheet (Fig. 7)
		40	0.0009	1750	1200	No. 3	
XIV	LRC-C22-S106	41	0.0003	1790	840	Helium	Start Up
		42	0.0009	1800	960	No. 3	Run Sheet (Fig. 9)
		43	0.0039	1800	900	No. 3	

TABLE 9 (Continued)

EXPERIMENT NO.	SPECIMEN IDENTIFICATION	RUN NO.	EXPERIMENTAL RUN CONDITIONS				REMARKS OR COMMENTS
			W (lb/ft^2-sec)	T_L (°F)	T_o (°F)	FEED BLEND	
XV	Graphite (Grade 25)	44	0.0003	1590	880	Helium	Start Up
		45	0.0009	1710	1125	No. 3	Analytical Problems
		46	0.0001	1755	1185	No. 3	
XVI	Low Density Phenolic-Nylon	47	0.0009	1880	740	Helium	Start Up
		48	0.0003	2015	1120	No. 3	
		49	0.00003	2055	1260	No. 3	Run Sheet (Fig. 10)
		50	0.0012	2035	1162	No. 3	
		51	0.0170	2035	1000	No. 3	
		52	0.0048	2035	990	No. 3	
XVII	Low Density Phenolic-Nylon	53	0.0050	2000	315	Helium	Start Up
		54	0.0350	2045	310	Air	Run Sheet (Fig. 11)

FIGURE 15 : RUN SHEET EXPERIMENT VII

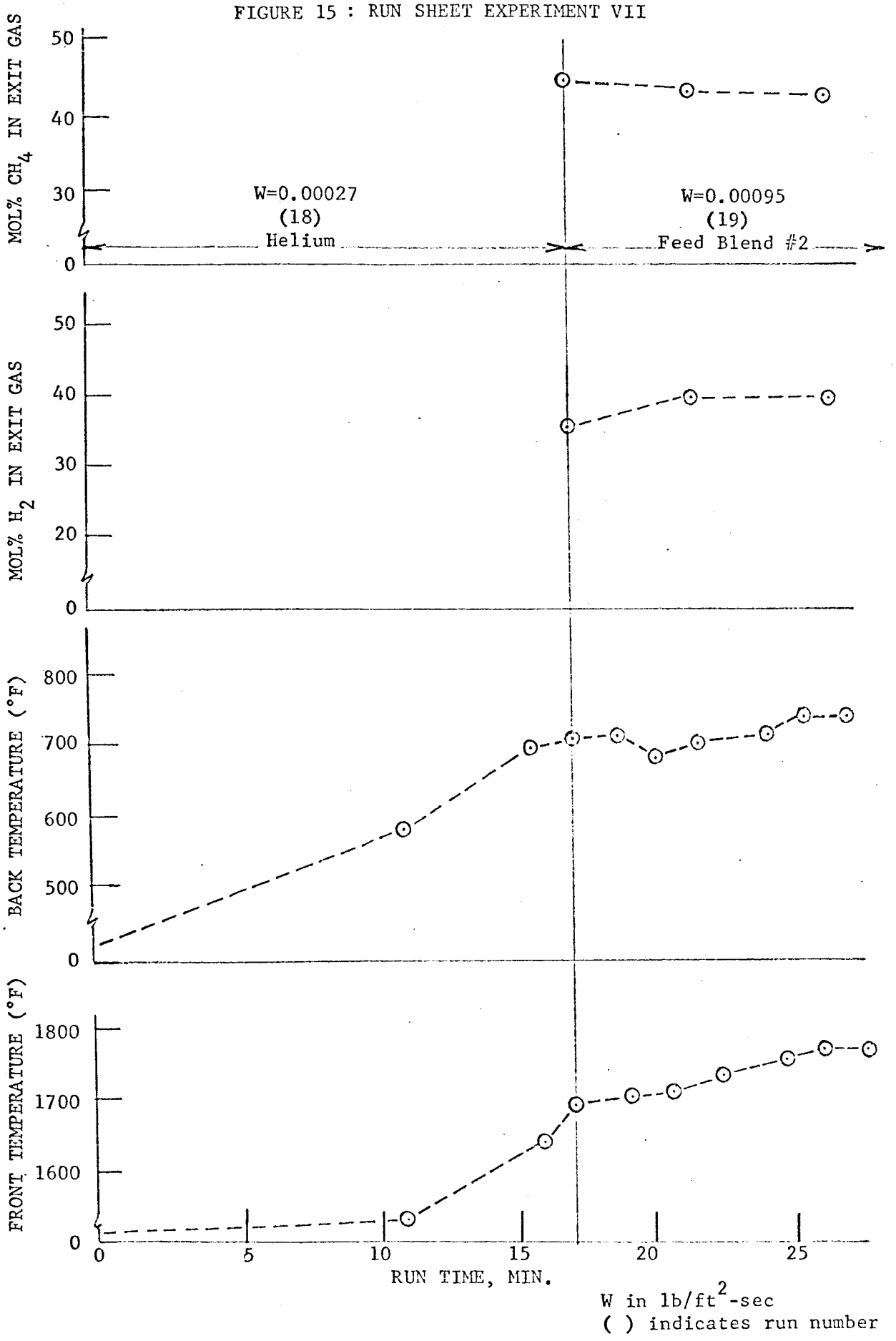

W in lb/ft^2-sec

( ) indicates run number

FIGURE 14: RUN SHEET EXPERIMENT IV

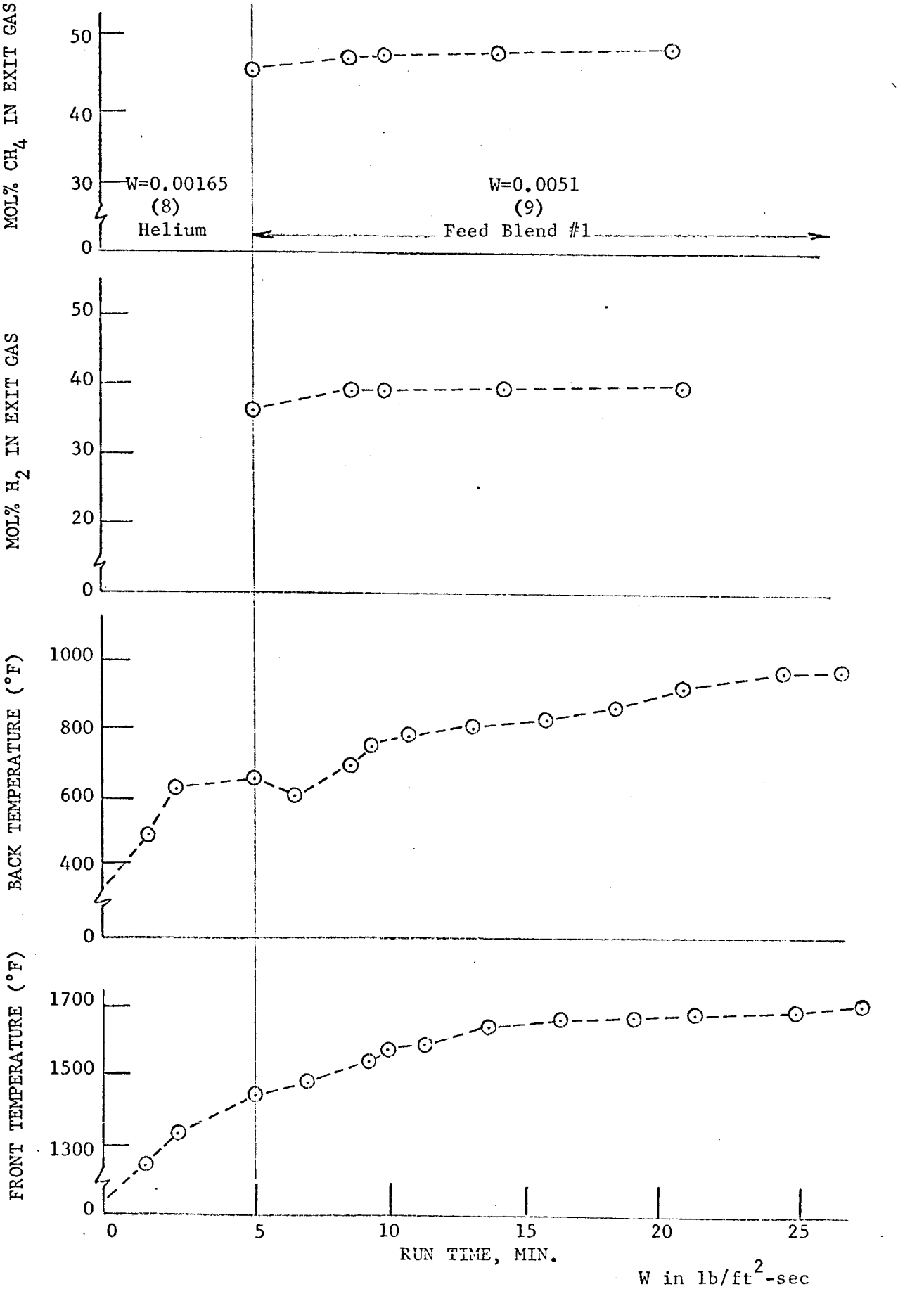

W in lb/ft^2-sec

( ) indicates run number

DISTRIBUTION

		Copies
1.	Headquarters Contracts Division, Code DHC-4 National Aeronautics and Space Administration Washington, D. C. 20546	10
2.	Structures Research Division Langley Research Center, N.A.S.A. Hampton, Virginia	2
3.	Mr. Robert T. Swann, Grant Monitor Entry Structures Branch M.S. 206 Langley Research Center, N.A.S.A. Hampton, Virginia	5
4.	Mr. Melvin G. Rosche, Chief Space Vehicle Structures Branch RV-2 National Aeronautics and Space Administration Washington, D. C. 20546	1
5.	Dr. Bernard G. Achhammer RRM - B 556 National Aeronautics and Space Administration Washington, D. C. 20546	1
6.	Mr. Fred J. DeMeritte, Chief Aeorthermchemistry Branch RV - 2 National Aeronautics and Space Administration Washington, D. C. 20546	1
7.	Mr. David A. Greenshields, Chief Thermal Technology Branch ES 5 Manned Spacedraft Center National Aeronautics and Space Administration Houston, Texas	1
8.	Mr. Bradford H. Wicks, Chief Gasdynamics Branch N 234-1 Ames Research Center Moffitt Field, California 94035	1
9.	Mr. Nick S. Vojvodich Gasdynamics Branch N 234-1 Ames Research Center, N.A.S.A. Moffitt Field, California 94035	1
10.	Dr. Roger W. Richardson, Dean College of Engineering Louisiana State University Baton Rouge, Louisiana 70803	1

11.	Dr. Paul W. Murrill, Head Department of Chemical Engineering Louisiana State University Baton Rouge, La. 70803	1
12.	Authors	3
13.	File	2
	Total copies	30